Electrical response of amorphous silicon thin-film transistors under mechanical strain

H. Gleskova[a] and S. Wagner
Department of Electrical Engineering and Center for Photonics and Optoelectronic Materials, Princeton University, Princeton, New Jersey 08544

W. Soboyejo and Z. Suo
Department of Mechanical and Aerospace Engineering, Princeton University, Princeton, New Jersey 08544

(Received 3 June 2002; accepted 16 August 2002)

We evaluated amorphous silicon thin-film transistors (TFTs) fabricated on polyimide foil under uniaxial compressive or tensile strain. The strain was induced by bending or stretching. The on-current and hence the electron linear mobility μ depend on strain ε as $\mu=\mu_0(1+26\times\varepsilon)$, where tensile strain has a positive sign and the strain is parallel to the TFT source-drain current path. Upon the application of compressive or tensile strain the mobility changes ''instantly'' and under compression then remains constant for up to 40 h. In tension, the TFTs fail mechanically at a strain of about $+0.003$ but recover if the strain is released ''immediately.'' © *2002 American Institute of Physics.* [DOI: 10.1063/1.1513187]

I. INTRODUCTION

Electronic paper, smart labels, displays for vehicles and hand-held devices, sensor skins, and electrotextiles often require flexible substrates. For these applications, the traditional glass substrate of large-area electronics must be replaced with foils of metals or organic polymers. Stainless steel foils are suitable as substrates for amorphous,[1] nanocrystalline, and poly-silicon thin-film transistors[2] without much change of present fabrication processes. Organic polymers come in a wide variety. Many are inexpensive and transparent in the visible part of the light spectrum. However, in thin-film electronics a whole range of substrate characteristics become important including chemical stability, high softening, or glass transition temperature, low coefficient of thermal expansion (comparable to that of the materials used for thin-film electronics), negligible shrinkage during circuit fabrication, small coefficient of humidity expansion, low solubility for water, low water and oxygen permeability, and small surface roughness. Polyimides meet many of these requirements well.

All flexible or conformal display applications require some degree of bending. Bending or draping will induce strain in the electronic circuits. Therefore, understanding the electrical performance of thin-film transistors (TFTs) during and after mechanical strain becomes essential.

Back-channel etch amorphous silicon thin-film transistors ($a-$Si:H TFTs) fabricated on 25-μm thick Kapton foil can be bent to very small radii of curvature.[3] However, they respond differently to compressive (inward cylindrical bending) or tensile strain (outward bending). Figure 1 depicts the on current, source-gate leakage current, threshold voltage, and electron mobility, normalized to their initial values, as a function of the applied strain. The TFT was subjected to the strain for one minute, then was released and evaluated in the relaxed state. Any *irreversible* change in the TFT transfer characteristic due to mechanical failure under compression or tension would be observed in this experiment. After compression, no change was observed in the TFT characteristics for strains smaller than ~-0.02 (bending radius of ~0.5 mm), while after tension, a change in the TFT characteristics was observed beginning at a strain of $\sim+0.005$ (bending radius of ~2 mm). Indeed, under excessive tention the TFTs failed. The failure mode was periodic crack formation in the TFT island, with the cracks running perpendicular to the bending direction.

In this article we present a study of the electrical behavior of $a-$Si:H TFTs fabricated on polyimide substrate *during* compressive or tensile strain. *Reversible* changes in the TFT transfer characteristics were observed, namely, the electron linear mobility μ decreases under compression (increases under tension) and then returns to the original value after the strain is released.

II. EXPERIMENTAL PROCEDURES

A key aspect of using organic polymers as substrates for TFT electronics is the initial surface passivation. The passivation layer ''seals'' the polymer foil and converts the chemistry of the polymer to the chemistry of the passivating material. Semiconductor devices are highly susceptible to contamination, and the passivation layer substantially reduces the chance of contamination of the TFT layers during their growth, caused by outgassing and oxygen and water release from the polymer foil. The passivation layer also serves as the mechanical bond between the TFT layers and the substrate.

During TFT fabrication, the polymer foil may be temporarily attached to a rigid substrate, such as a silicon or glass wafer, or used as a free-standing substrate.[4–10] If it is attached, the thermal expansion of the compliant foil substrate during temperature cycling will be constrained to the stiff

[a]Electronic mail: gleskova@ee.princeton.edu

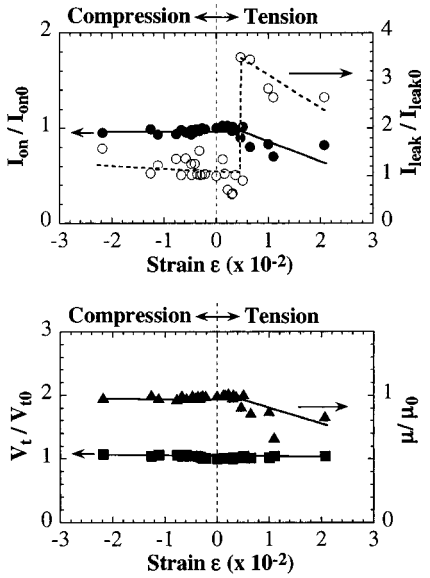

FIG. 1. On current I_{on}, source-gate leakage current I_{leak}, threshold voltage V_t, and electron mobility μ of $a-$Si:H TFTs on 25-μm polyimide substrates after 1 min of cylindrical deformation and release, normalized to their values before deformation.[3]

glass (coefficient of thermal expansion $\alpha = 3.76\times10^{-6}/°C$ for Corning 1737 glass) or Si wafer ($\alpha = 2.5\times10^{-6}/°C$). After fabrication the polymer foil, which now carries the TFTs, is detached from the rigid substrate. Our TFT fabrication process uses a 51-μm thick free-standing polymer foil. Therefore, its coefficient of thermal expansion must match that of the TFT layers reasonably well and the built-in stress in all TFT layers must be very well controlled. Otherwise, severe substrate curving may occur.

The polyimide Kapton®E works well as a substrate for $a-$Si:H TFT fabrication. It is stable to the TFT process chemicals, has a glass transition temperature $>350\,°C$, a coefficient of thermal expansion of $12\times10^{-6}/°C$,[11] and an root-mean-square surface roughness of ~30 nm.[9] A 51-μm thick foil shrinks $\sim0.04\%$ after 2 h at 200 °C, it has the relatively low humidity expansion coefficient of $9\times10^{-6}/\%RH$, a water permeability of 4 g/m^2/day, and an oxygen permeability of 4 cm^3/m^2/day.[11]

We fabricated arrays of $a-$Si:H TFTs at 150 °C on a free-standing Kapton E substrate passivated on both sides with SiN_x deposited by plasma enhanced chemical vapor deposition (PECVD). The standard $a-$Si:H TFT process temperatures lie between 250 and 350 °C. We reduced the temperature to 150 °C (Ref. 12) for two reasons: (i) several other polymers can withstand the temperature of 150 °C (Ref. 13) and therefore a 150 °C TFT technology can be used on other substrates, and (ii) $a-$Si:H and SiN_x layers grown by PECVD at 150 °C can be grown with a quality comparable to the materials grown at standard temperature.[12]

The TFTs have the inverted, bottom gate staggered geometry with SiN_x back-channel passivation. The polyimide substrate foil is first coated on both sides with a 0.5-μm thick layer of SiN_x. All TFTs have the following structure: $\sim$100-nm thick Ti/Cr layer as gate electrode, $\sim$360 nm of gate SiN_x, $\sim$100 nm of undoped $a-$Si:H, 180 nm of passivating SiN_x, $\sim$50 nm of (n^+) $a-$Si:H, and $\sim$100-nm thick Al for the source-drain contacts. Fabrication details are given elsewhere.[12] The channel length is 40 μm and the channel width 400 μm. Figure 2 is a cross-sectional view of this structure. After fabrication, the SiN_x layer on the back of the substrate is etched away and the transistors are annealed in forming gas. Figure 3 shows typical transfer characteristics for these devices. The off current is $\sim3\times10^{-12}$ A, the on-off current ratio $>10^6$, the threshold voltage ~3 V, and the subthreshold slope ~0.5 V/decade. The electron linear mobility, calculated from the transfer characteristic for drain-to-source voltage $V_{ds}=0.1$ V, is ~0.45 cm^2/Vs.

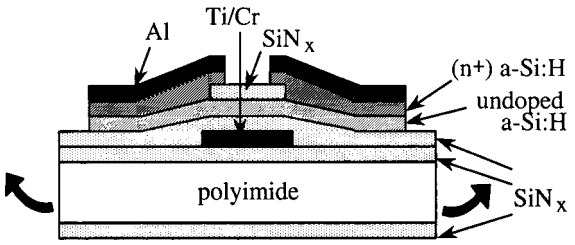

FIG. 2. Cross section of $a-$Si:H TFT fabricated on $\sim$51-μm thick polyimide foil. The arrows denote the bending direction parallel with the TFT source-drain current path.

We strained the transistors by either bending or stretching. Inward cylindrical bending produces compression, by definition negative, and outward bending tension, positive. The bending direction in most cases was parallel to the source-drain current path, as shown by the heavy arrows in Fig. 2. A few TFTs were also tested with the bending direction perpendicular to the source-drain current path. In compression, single TFTs were bent to various radii of curvature R, ranging from 70 to 1.6 mm. Transfer characteristics like those of Fig. 3 were measured at each bending radius. Some TFTs were measured at several R, while others were bent permanently to a fixed R, to monitor the change in the transfer characteristics for $\sim$40 h.

From each set of transfer characteristics, we extracted the off-current I_{off}, on-current I_{on}, gate leakage current I_{leak}, linear mobility μ, threshold voltage V_t, and subthreshold slope S. The definition of these currents is as follows: The off-current is the smallest drain-to-source current at $V_{ds}=10$ V, the on-current is the drain-to-source current for V_{ds}

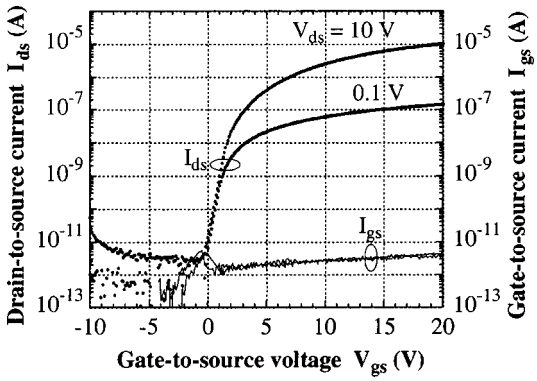

FIG. 3. Transfer characteristics for the TFT of Fig. 2. The source is grounded.

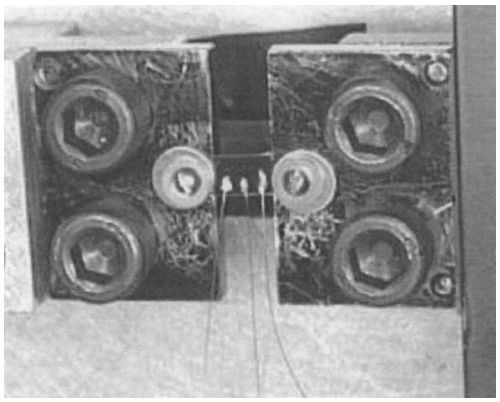

FIG. 4. Photograph of an individual $a-$Si:H TFT stretched in a microstrain tester and wired for electrical evaluation.

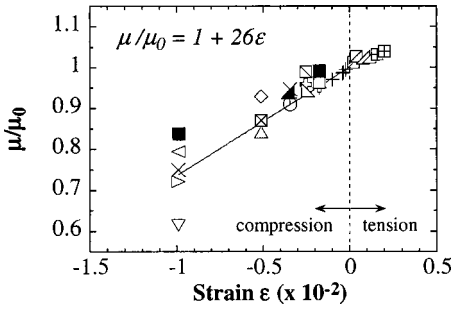

FIG. 5. Relative mobility plotted as a function of strain. Each symbol represents a different TFT. Empty and full symbols correspond to TFTs with the bending direction parallel and perpendicular to the source-drain current path, respectively. The linear fit is for TFTs with the bending direction parallel to the source-drain current path.

$=10$ V and $V_{gs}=V_t+10$ V, and the leakage current is the gate-to-source current for $V_{ds}=10$ V and $V_{gs}=20$ V. V_t and μ were calculated from the transfer characteristic for $V_{ds}=0.1$ V, while S was obtained by fitting an exponential function to the subthreshold region of the transfer characteristic for $V_{ds}=10$ V. To obtain reference values for these parameters, each TFT was measured first before any strain was applied. We calculated the strain at the $SiN_x/a-$Si:H interface of the TFTs using Eq. (1) of Ref. 3. Young's modulus of our polyimide substrate is 5 GPa (Ref. 11) and we assumed 183 GPa for all TFT layers.[14] The highest compressive strain, at the smallest bending radius of $R=1.6$ mm, was ~ -0.01, the highest tensile strain was $\sim +0.002$.

Additional $a-$Si:H TFTs were subjected to uniaxial tensile strain in a microstrain tester as shown in Fig. 4. Individual TFTs were firmly clamped between two jaws, one stationary and one movable, of the tester. A controlled load was applied to the movable jaw and measured with a load cell. The stretching direction was parallel to the source-drain current path. Transfer characteristics like those of Fig. 3 were measured for each load (tensile stress), via gold wires soldered with indium to the source, drain, and gate contact pads (see Fig. 4). From each set of transfer characteristics we extracted I_{off}, I_{on}, I_{leak}, μ, V_t, and S using the method described above. The configuration of the microstrain tester allowed measurements only under tension.

To compare the data from the bending and stretching experiments, we calculated the strain ε under stretching from the known load F using the following formula:

$$\varepsilon = \frac{F}{Y_f A_f + Y_s A_s}, \tag{1}$$

where Y_f and Y_s are Young's moduli of the film and the substrate, respectively, and A_f, A_s are the cross-sectional areas of the two materials. The values for Y_f and Y_s are given above. Equation (1) assumes a linear relationship between stress and strain (elastic deformation), which in our experience is a reasonable assumption for $a-$Si:H TFTs on polyimide substrates. The strains that we calculate are first-order values, because they consider neither lateral constraint of the substrate nor variations in transistor cross-sections. Eventually more precise, numerical, calculations will be needed to evaluate locally varying strain in specific device and circuit geometries.

III. RESULTS AND DISCUSSION

A. Compressive and tensile strain induced by bending

We first applied *compressive* strain and observed a slight decrease in the on-current I_{on}, and hence the linear mobility μ. The changes in the off-current I_{off} and leakage current I_{leak} remained within experimental error and we concluded that they did not change. There was a substantial scatter in the threshold voltage V_t and subthreshold slope S. While no clear conclusion could be made about V_t, S seemed to rise slightly with increasing compressive strain. Next, we applied increasing *tensile* strain and observed that the linear mobility μ did increase while the subthreshold slope S remained unchanged.

Figure 5 depicts the relative mobility μ/μ_0 as a function of strain ε, where μ is the linear mobility under an imposed strain and μ_0 is the initial linear mobility. Each symbol on the graph represents a different TFT. The empty and full symbols correspond to TFTs with the parallel and perpendicular bending direction, respectively. There is no qualitative difference in the behavior of μ/μ_0 as a function of direction of the strain, but quantitatively the values of μ/μ_0 remain slightly larger in the perpendicular bending direction. A linear fit to mobilities measured under parallel bending direction gives: $\mu/\mu_0=1+26\times\varepsilon$.

Figure 6 shows the relative subthreshold slope S/S_0, where S is the subthreshold slope at a given strain and S_0 is the initial slope. While there is a clear trend in μ/μ_0 as a function of strain ε, the spread in S/S_0 is quite large. The solid line in Fig. 6, which is a linear fit to the experimental data, indicates that there is a decrease in S/S_0 with the applied strain, but we draw this conclusion with some reservation.

For a given strain, the change in the mobility was 'instantaneous' to a new value that remained constant during the measurement time of ~ 40 h. (Since it takes several minutes to measure the transfer characteristics, the measured mobility reflects the situation several minutes after the strain

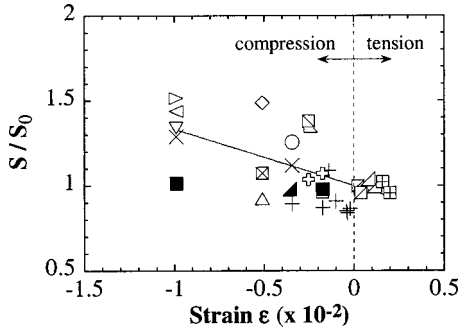

FIG. 6. Relative subthreshold slope plotted as a function of strain. Symbols as in Fig. 5.

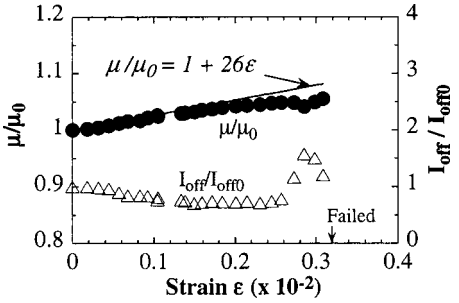

FIG. 8. Relative mobility and off-current plotted as functions of tensile strain. The TFTs were stretched along the direction of the source-drain current path.

has been applied.) Figure 7 shows the mobility μ/μ_0, the off-current $I_{\text{off}}/I_{\text{off0}}$, and the leakage current $I_{\text{leak}}/I_{\text{leak0}}$ as functions of time during which $\varepsilon=-0.01$ compressive strain was applied. As mentioned above, no change in the off current or leakage current was observed and therefore $I_{\text{off}}/I_{\text{off0}}$ and $I_{\text{leak}}/I_{\text{leak0}}$ remain unity.

B. Tensile strain induced by uniaxial stretching

Figures 8 and 9 show an example of the effect of tensile strain applied in the strain tester on $a-$Si:H TFT characteristics when the TFT is strained along the channel length. The load was increased in small increments up to the breaking point. Figure 8 depicts the relative mobility and off-current. Initially, the mobility increases as a function of strain and follows the same dependence as observed in the bending experiment. For strains larger than $\sim+0.002$, the mobility starts to deviate from this behavior. The off-current slowly decreases up to the strain of $\sim+0.0025$ and then it rises to a peak just before the TFT fails mechanically. However, several TFTs showed no change in the off-current. Figure 9 shows the relative change in the threshold voltage V_t and the subthreshold slope S. The threshold voltage slowly increases, while the subthreshold slope exhibits behavior similar to the off-current. All TFT parameters display unusual behavior when the tensile strain approaches the failure strain. For now we conclude that the increase in the threshold voltage reflects the usual dangling-bond instability of $a-$Si:H TFTs since V_t always rises even when the tensile strain is gradually decreased. Further investigation is necessary to determine if the strain has an effect on the magnitude of the threshold voltage shift.

Several TFTs failed at the strain of $\sim+0.003$. Interestingly enough, if the tensile strain of the failed TFT was ''immediately'' reduced to zero, the TFT transfer characteristics returned to normal. This is documented in Fig. 10, which shows the initial transfer characteristics of a virgin TFT, then the characteristics of the same TFT at the failure strain, and again after the strain was released. The transfer characteristics do not show any signs of the previous failure and one cannot distinguish them from those of a virgin TFT. The TFTs can be cycled through the failure and recovery process several times before they start to show permanent changes in their transfer characteristics. The parameter that affects the number of the failure-recovery cycles is the time for which the TFT is kept under failure strain. If the TFT is held at failure strain for several hours, it never recovers.

SEM analysis combined with optical microscopy revealed that the Ti/Cr gate line inside of the TFT structure does crack but the crack does not propagate easily in any direction. This is not surprising since Cr is not ductile and has built-in tensile strain. Once the strain is released the crack ''closes'' and the TFT cannot be distinguished from a virgin TFT. The only sign of previous failure is the reduction in the failure strain as the number of the failure-recovery cycles is increased.

The failure strain of $\sim+0.003$ is lower than previously reported.[3] A tensile strain larger than $\sim+0.003$ but smaller than $\sim+0.005$ causes mechanical failure of the TFT, but this failure is observed only if the TFT is measured while strained, or after having been kept at the failure strain for a

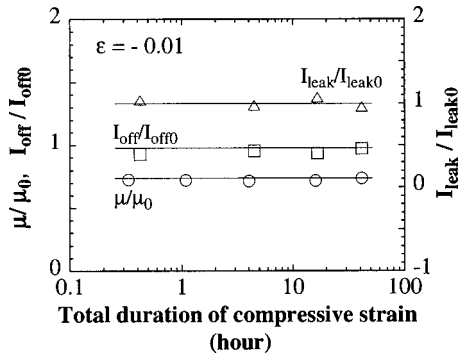

FIG. 7. Relative mobility, off-current, and leakage current as functions of duration of an applied compressive strain of ~-0.01.

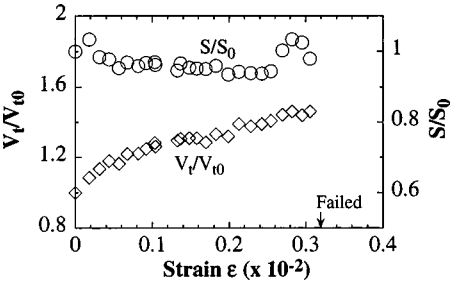

FIG. 9. Relative threshold voltage and subthreshold slope plotted as functions of tensile strain. Stretching direction as in Fig. 8.

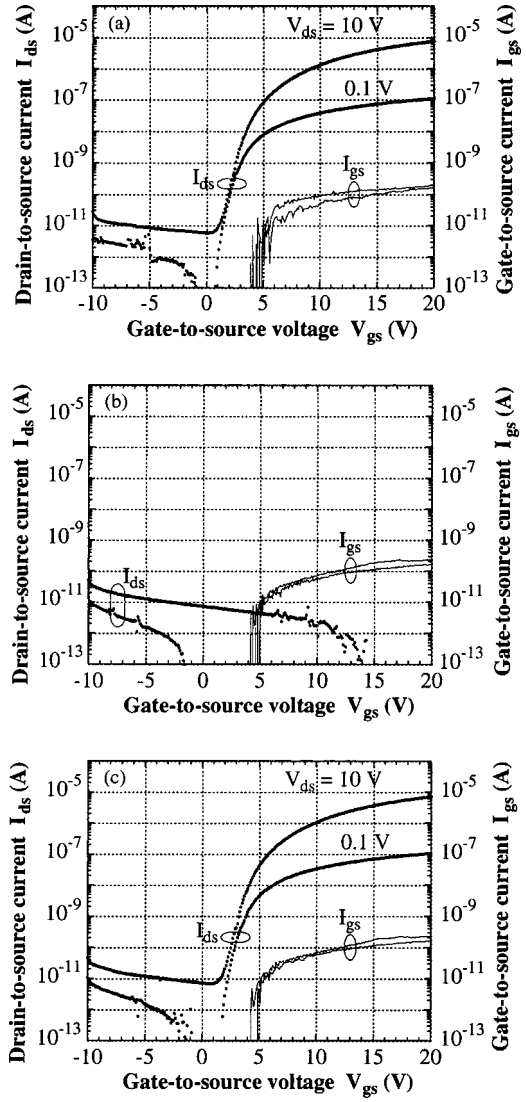

FIG. 10. Transfer characteristics of a virgin TFT (a), characteristics of the same TFT at the failure strain (b), and again after the strain is released (c).

prolonged time. Otherwise, the TFT is highly likely to recover to the original performance after the strain is removed.

C. Why is the electron field-effect mobility strain dependent?

The behavior of the field-effect mobility of $a-$Si:H TFTs under strain is similar to the changes in the dark conductivity of undoped and n-type doped $a-$Si:H films due to the piezoresistive effect.[15] The conductance of undoped and (n^+) $a-$Si:H material increases (decreases) with increasing uniaxial tensile (compressive) strain. The magnitude of the conductance depends on the directions of the applied strain and the current path with respect to each other. The maximum change occurs when the strain is parallel to the current path, the minimum change occurs when the strain is perpendicular to the current path. The mobility in our $a-$Si:H TFTs under uniaxial strain qualitatively follows the same behavior. The mobility increases in tension (up to the failure strain) and decreases under compression. The change in the mobility is larger for TFTs where the strain is parallel to the source-drain current path than for TFTs where the strain is perpendicular to the source-drain current path. This behavior also is qualitatively similar to the one observed in uniaxial, tensile-strained, crystalline silicon metal-oxide-semiconductor field-effect transistors (MOSFETs), however $a-$Si:H TFTs exhibit substantially smaller change in the mobility.[16]

Because the $a-$Si:H TFT is a complex device consisting of several layers, we have found it difficult to clearly trace the changes in the current-voltage characteristics to their physical origin. On one hand, the piezoresistive effect in undoped and n-type doped $a-$Si:H affects the contact resistance and hence the on-current and therefore the apparent field-effect mobility. On the other hand, any change in the band gap, the slope of the conduction-band tail, or the dangling bond density of the $a-$Si:H channel material also will affect the mobility. In $a-$Si:H TFTs, the free electron mobility, which is set by scattering on every silicon atom, is reduced to an effective mobility by frequent trapping in the conduction-band tail states of $a-$Si:H channel material. The slopes of the conduction- and valence-band tails are correlated[17,18] and controlled by the amount of structural and/or thermal disorder.[19] The band gap of $a-$Si:H is also affected by disorder[19] and it decreases with increasing hydrostatic pressure.[20] We have linked the reduction of the optical band gap of intrinsic $a-$Si:H under compression via the experimental results of Refs. 17–20 to the changes observed in the TFT field-effect mobility under compression. The two effects agree within a factor of two.[21] Further study is needed to determine the primary mechanism causing the reversible mobility changes and to detect concurrent changes in the off-current, the threshold voltage, and the subthreshold slope.

IV. CONCLUSIONS

We applied uniaxial strain ranging from -0.01 to $\sim+0.003$ to $a-$Si:H TFTs on polyimide foil by bending them inward or outward, or by stretching them in a microstrain tester. The bending direction was either parallel or perpendicular to the source-drain current path. The stretching direction was parallel to the source-drain current path. Compression produced a decrease, while tension caused an increase in the on-current and hence the linear mobility (except if the tensile strain exceeded the failure strain). The change in the mobility was ''instantaneous'' on the time scale of several minutes and the mobility increased linearly with the applied strain. In compression, the mobility did not change further for stress duration of up to 40 h. The change in the mobility qualitatively agrees with earlier observations of the piezoresistive effect in $a-$Si:H, and it appears to be caused by the changes in the slope of the conduction-band tail of the $a-$Si:H channel material.

The failure strain under tension was found to be $\sim+0.003$, a lower value than we previously reported. A tensile strain larger than $\sim+0.003$ but smaller than $\sim+0.005$ causes mechanical failure of the TFT, but this failure is observed only if the TFT is measured while strained, or after having been kept at the failure strain for a prolonged time. If the TFT is relaxed soon, it is highly likely to recover to the original performance after the strain is removed.

ACKNOWLEDGMENTS

We gratefully acknowledge support from DARPA, NSF, and the New Jersey Commission on Science and Technology.

[1] S. D. Theiss and S. Wagner, IEEE Electron Device Lett. **17**, 264 (1996).
[2] M. Wu, K. Pangal, J. C. Sturm, and S. Wagner, Appl. Phys. Lett. **75**, 2244 (1999).
[3] H. Gleskova, S. Wagner, and Z. Suo, Appl. Phys. Lett. **75**, 3011 (1999).
[4] G. N. Parsons, C. S. Yang, C. B. Arthur, T. M. Klein, and L. Smith, Mater. Res. Soc. Symp. Proc. **508,** 19 (1998).
[5] H. Gleskova, S. Wagner, and Z. Suo, Mater. Res. Soc. Symp. Proc. **508,** 73 (1998).
[6] J. N. Sandoe, in *1998 SID International Symposium, Digest of Technical Papers*, Vol. 29, edited by J. Morreale, (Society for Information Display, Santa Ana, CA, 1998), pp. 293–296.
[7] E. Lueder, M. Muecke, and S. Polach, in *Proceedings of the 18th International Display Research Conference, Asia Display '98*, edited by Jin Jang, (Society for Information Display, Santa Ana, CA, 1998), pp. 173–177.
[8] A. Constant, S. G. Burns, H. Shanks, C. Gruber, A. Landin, D. Schmidt, C. Thielen, F. Olympie, T. Schumacher, and J. Cobbs, Electrochem. Soc. Proc. **94–35**, 392 (1995).
[9] D. B. Thomasson, M. Bonse, J. R. Huang, C. R. Wronski, and T. N. Jackson, in *International Electron Devices Meeting-1998* (IEEE Technical Digest, Piscataway, NJ, 1998), pp. 253–256.
[10] S. D. Theiss, P. G. Carey, P. M. Smith, P. Wickboldt, T. W. Sigmon, Y. J. Tung, and T.-J. King, in *International Electron Devices Meeting-1998* (IEEE Technical Digest, Piscataway, NJ, 1998), pp. 257–260.
[11] J. A. Kreuz, S. N. Milligan, and R. F. Sutton, DuPont Films Technical Paper 3/94, Reorder No. H-54504.
[12] H. Gleskova, S. Wagner, V. Gašparík, and P. Kováč, J. Electrochem. Soc. **148**, G370 (2001).
[13] S. M. Gates, Mater. Res. Soc. Symp. Proc. **467,** 843 (1997).
[14] F. Jansen and M. A. Machonkin, J. Vac. Sci. Technol. A **6**, 1696 (1988).
[15] W. E. Spear and M. Heintze, Philos. Mag. B **54**, 343 (1986).
[16] R. E. Belford, J. Electron. Mater. **30**, 807 (2001).
[17] S. Sherman, S. Wagner, and R. A. Gottscho, Appl. Phys. Lett. **69**, 3242 (1996).
[18] S. Sherman, P. Y. Lu, R. A. Gottscho, and S. Wagner, Mater. Res. Soc. Symp. Proc. **377,** 749 (1995).
[19] G. D. Cody, T. Tiedje, B. Abeles, B. Brooks, and Y. Goldstein, Phys. Rev. Lett. **47**, 1480 (1981).
[20] B. Welber and M. H. Brodsky, Phys. Rev. B **16**, 3660 (1977).
[21] H. Gleskova and S. Wagner, Appl. Phys. Lett. **79**, 3347 (2001).